Part II

Magnetized stellar winds

Chapter 3

The solar wind

A fool sees not the same tree that a wise man sees
No bird soars too high if he soars with his own wings
If the fool would persist in his folly he would become wise
What is now proved was once only imagin'd

William Blake
The Marriage of Heaven and Hell (1793)

Like rotation and magnetic fields, mass loss is rather ubiquitous across the Herztsprung-Russell diagram. Some stars lose mass in an episodic, often spectacular manner, but most do so more calmly, via a **wind** emanating from their surface. Many different physical mechanisms can power a wind, and guess what, magnetic fields often plays an important part in many of them, as we will explore in the following two chapters. But first we need to establish our baseline wind theory, pertaining to unmagnetized, thermally-driven winds, and towards this goal the Sun is the best starting point, because its wind can be sampled and measured *in situ* by Earth-orbiting satellites.

3.1 Solar and stellar coronae and winds

3.1.1 The solar corona

The story of the solar wind is intimately tied to that of the **solar corona**. The corona being spectacularly visible at times of solar eclipses (see Figure 3.1), we can safely assume that it was first observed a very long time ago by some hairy Neanderthal with smelly armpits and questionable table manners. Its first unambiguous description (of the corona, not the Neanderthal) is due to the Byzantine chronicler Leo Diaconus (ca. 950-994) who, after witnessing the 22 December 968 solar eclipse, reports:

> "...at the fourth hour of the day ... darkness covered the Earth and all the brightest stars shone forth. And is was possible to see the disk of the Sun, dull and unlit, and a dim and feeble glow like a narrow band shining in a circle around the edge of the disk.".

Only by the early decades of the eighteenth century had most astronomers finally convinced themselves that the corona was part of the sun, rather than the moon. The actual name "corona" was coined even later, in 1806, by the Spanish astronomer José Joachin de Ferrer. By the nineteenth century it had become a rite of passage for solar physicists to travel to faraway corners of the Earth to observe solar eclipses, a tradition still very much alive today.

Despite rapid advances in spectroscopic and photographic techniques in the second half of the nineteenth century, the physical nature of the corona remained a mystery until the development of the coronagraph by Bernard Lyot (1897-1952) in the early 1930's allowed systematic

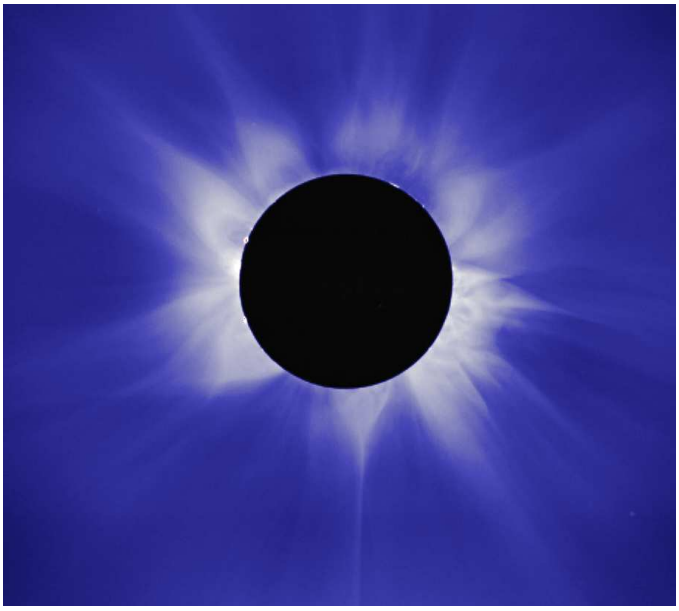

Figure 3.1: Total solar eclipse of 16 February 1980, essentially at the maximum phase of the solar activity cycle. Coronal brightness is due to Thompson scattering of sunlight by free electrons, so that on such images brightness is proportional to plasma density. The elongated spiky structures are called helmet streamers, and correspond to regions of closed magnetic fields trapping plasma, eventually pulled open and stretched radially by the solar wind a solar radius or so above the photosphere. Image courtesy of A. Stanger, High Altitude Observatory.

studies of the corona outside eclipses. By the late 1930's, mostly through the laboratory work of of Walter Grotrian (1890-1954) and Bengt Edlén (1906-1993), the solar corona was recognized as being composed of very hot (1–2$\times 10^6$ K) ionized gas. The key in reaching that conclusion was the realization that many of the hitherto unidentified lines seen in coronal spectra were not due to chemical elements unknown on Earth, as believed for a while in the nineteenth century, but rather belonged to high ionization stages of common elements, notably Iron and Nickel. The mechanism(s) through which the corona can be heated to such high temperatures remains, to this day, one of the grand unsolved problems of solar physics. Moreover, like if a few million degrees K wasn't hot enough already, the corona harbors even hotter plasma, at temperatures sometimes reaching 10 million degrees during transient events called flares (see Fig. 2.5).

The peculiar flame-like structures so prominently visible on eclipse photographs such as Fig. 3.1, called **helmet streamers**, are produced by large-scale loop-like magnetic structures emanating from the solar photosphere and trapping the ionized coronal plasma (flux-freezing, remember...). This leads to overdensities in magnetically closed regions of the corona, leading to enhanced Thompson scattering of sunlight, and thus enhanced brightness. The shape of the solar corona varies according to the distribution of photospheric magnetic fields (viz. Fig. 2.4). This can eventually break the dynamical equilibrium of helmet streamers, and lead to coronal mass ejections (see Fig. 2.6).

The take-home message, at this point, is that there is a hot corona out there, and that it is structured at all spatial scales by the solar magnetic field.

3.1.2 The solar wind

The existence of an outflow of matter from the Sun was suggested at the end of the nineteenth century by the Norwegian physicist Kristian Birkeland (1867-1917), as an explanation for geomagnetic storms (in particular auroral emission) and zodiacal light. Indeed, by 1899 Birkeland

had convinced himself (but unfortunately not a great many others) that interplanetary space is filled with electrically charged particles streaming away from the Sun. The idea did not catch on at the time, but was brought back to the fore half a century later by Ludwig Biermann (1907-1986), as an explanation for the different orientations of neutral and ionized components of cometary tails.

The first quantitative, physical model of what we now call the **solar wind** was proposed in 1958 by Eugene Parker, and led to the surprising prediction that the solar wind should have a supersonic speed at the Earth's orbit. This was spectacularly confirmed by the first *in situ* measurements carried out by the Earth-orbiting satellites Lunik 2 (1960), Explorer 10 (1961), and Mariner 2 (1962). Later generations of space probes have now measured solar wind properties out to the far reaches of the solar system (in particular *Pioneer* and *Voyager*), as well as close to the Sun and away from the ecliptic plane (*Ulysses*).

The physical properties of the solar wind vary significantly on a broad range of timescales; as one can verify from the data summarized in the first columns of Table 3.1 below, at 1 AU fluctuations about the mean are quite large. These large fluctuations are not due to measurements errors. Examination of the distributions of deviations about the mean yields not a Gaussian, but rather a bimodal distributions, indicating that the solar wind exists in two distinct modes, dubbed "low-speed streams" and "high-speed streams". Separating the data in two groups then leads to much smaller deviations about the mean (rightmost columns on Table 3.1). It is now understood that low-speed streams originate from regions of the corona where the magnetic field is mostly closed (two footpoints on the photosphere), while high-speed streams originate from coronal holes, where the magnetic field is "open", i.e., fieldlines have one footpoint on the photosphere and extend from the solar surface all the way out into the solar system. This was spectacularly demonstrated by the measurements carried out by the space probe *Ulysses* near solar activity minimum, when the solar corona assumes a dipolar shape, with large coronal holes spanning the high heliospheric latitudes in both the Northern and Southern solar hemispheres (see Figure 3.2).

Table 3.1
Observed properties of the solar wind in the ecliptic plane at 1 AU

Quantity	Average	Low-speed	High-speed
N $[10^6\,\mathrm{m}^{-3}]$	8.7±6.6 (76%)	11.9±4.5 (38%)	3.9±0.6 (15%)
u $[\mathrm{km\,s}^{-1}]$	468±116 (25%)	327±15 (5%)	702±32 (5%)
Nu $[10^{12}\,\mathrm{m}^{-2}\mathrm{s}^{-1}]$	3.8±2.4 (63%)	3.9±1.5 (38%)	2.7±0.4 (15%)
ϕ_v (degrees)	−0.6±2.6 (430%)	+1.6±1.5 (94%)	−1.3±0.4 (31%)
T_p $(10^5\,\mathrm{K})$	1.2±0.9 (75%)	0.34±0.15 (44%)	2.3±0.3 (13%)
T_e $(10^5\,\mathrm{K})$	1.4±0.4 (29%)	1.3±0.3 (20%)	1.0±0.1 (8%)
T_α $(10^5\,\mathrm{K})$	5.8±5.0 (86%)	1.1±0.8 (68%)	14.2±3.0 (21%)

The last three lines of Table 3.1 list the (kinetic) temperatures inferred for protons, electrons and He nucleii, the most abundant constituents in the solar wind plasma. These are kinetic temperatures, obtained basically by measuring the randomly oriented component v of particle speeds and setting

$$kT = \frac{1}{2}mv^2 \ . \tag{3.1}$$

The fact that kinetic temperatures turn out considerably different for protons and Helium nucleii indicates that the plasma is no longer collision-dominated, meaning we are approaching the limit of our fluid approximation.

On very short timescales (seconds to minutes), there exist a wide spectrum of fluctuations in all wind variables (flow speed, magnetic field strength and orientation, density, etc.). Based on the type of correlations determined between these various fluctuating variables, a good case can

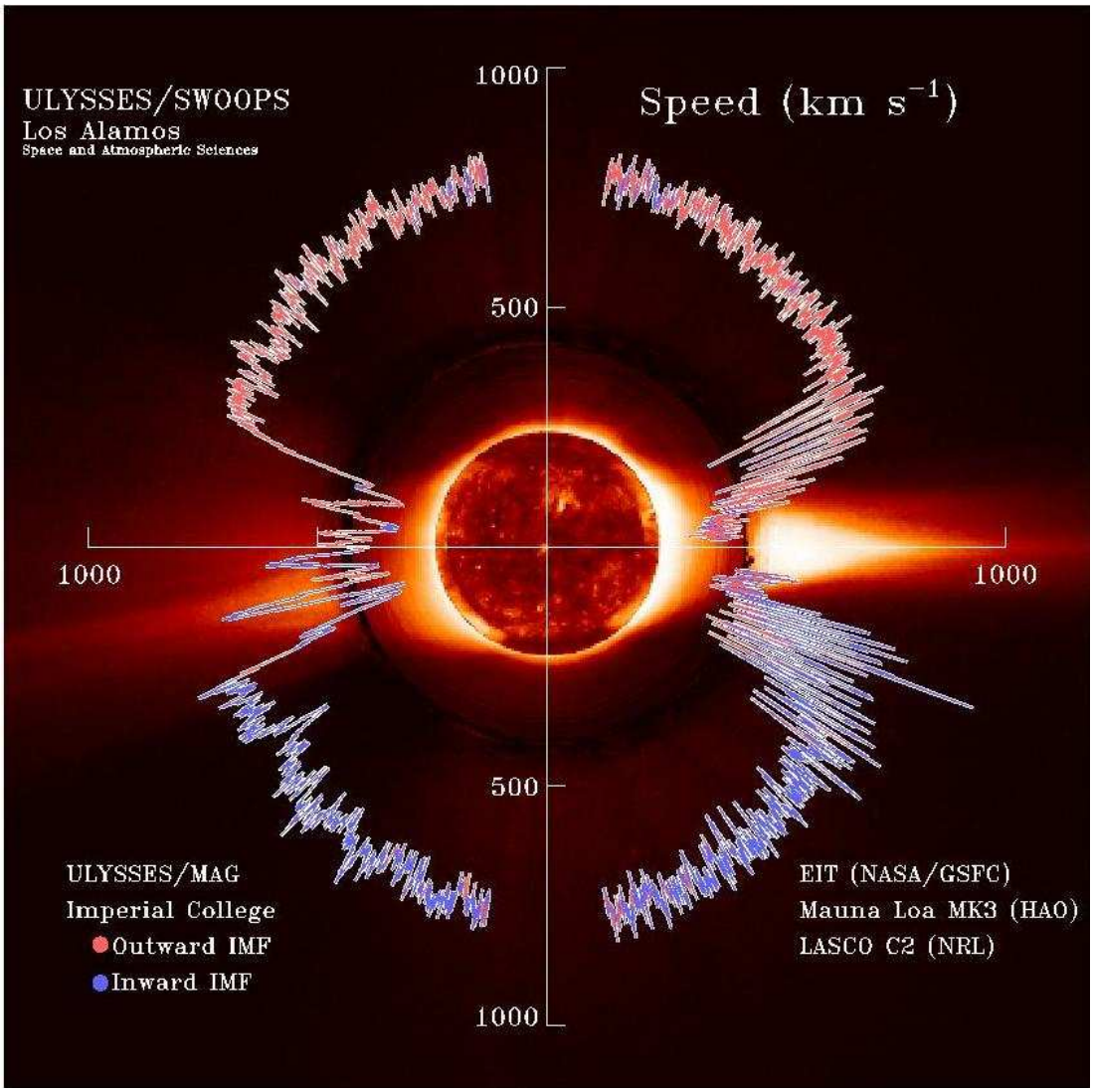

Figure 3.2: Image of the solar corona, on which is superposed a polar coordinate plot of the solar wind speed as measured approximately at 1.5 AU by the space probe *Ulysses*. The colors blue/red code the sign of the radial component of the magnetic field measured in the wind. This coronal/wind configuration is typical of activity minimum conditions, with the large-scale coronal magnetic field assuming a dipolar configuration, with a more or less axisymmetric helmet streamer belt straddling the solar equator. The faster wind component emanates from polar coronal holes, where magnetic fieldlines stretch directly out into interplanetary space.

be made that they correspond to a superposition of various type of magnetic and magnetosonic waves (briefly discussed in §1.5). The only type of waves for which a good case can be made for a solar origin are Alfvén waves, and these in fact can have a significant influence on wind dynamics, a topic to be revisited in due time. This is because numerous physical processes could generate waves in the expanding wind itself, and in the low density environment of the expanding solar wind, wave-particles interactions are guaranteed to alter the properties of any outgoing wave superimposed on the background flow. On the other hand, the power-law form of the fluctuation spectra is suggestive of turbulence, and an equally good case can be made that MHD turbulence should develop in the solar wind, even if the wind outflow is purely laminar at the coronal base.

3.2 Hydrostatic Corona Model

Since it is an observational fact that there *is* a hot corona out there, our task is now to construct a model allowing us to interpret these observations in a quantitative and coherent way. We start with a simple model, which is almost always a good idea. We assume that the corona is static ($\mathbf{u} = 0$), in a steady-state ($\partial/\partial t = 0$), spherically symmetric ($\partial/\partial\theta = 0$, $\partial/\partial\phi = 0$, $\partial/\partial r \to \mathrm{d}/\mathrm{d}r$), and unmagnetized ($\mathbf{B} = 0$). We construct a solution above a reference radius r_0, at which the density (ρ_0) and temperature (T_0) are assumed known. We also assume that the corona is composed only of fully ionized hydrogen ($m = m_p = 1.67 \times 10^{-27}$ kg, $\mu = 0.5$) obeying the equation of state for a perfect gas.

The r-component of the equations of motion becomes a simple statement of hydrostatic balance:

$$\frac{\mathrm{d}p}{\mathrm{d}r} = -\rho\frac{GM}{r^2}, \tag{3.2}$$

where we have assumed a spherically symmetric gravitational potential $\Phi = -GM/r$. This says nothing more that the (outward-directed) pressure gradient balances exactly the (inward-directed) gravitational acceleration, a particularly simple form of force balance. Assume now that a polytropic relationship[1] exists between the pressure and density:

$$\frac{p}{p_0} = \left(\frac{\rho}{\rho_0}\right)^{\alpha} . \qquad 1 \le \alpha \le 5/3 \tag{3.3}$$

Using for conciseness the definition of the base polytropic sound speed $c_{s0}^2 = \alpha p_0/\rho_0 = \alpha k T_0/\mu m$ for a perfect gas, eq. (3.2) now becomes

$$c_{s0}^2 \left(\frac{\rho}{\rho_0}\right)^{\alpha-1} \mathrm{d}\rho = -\rho\frac{GM}{r^2}\mathrm{d}r \ , \tag{3.4}$$

which is readily integrated to yield an expression for the density profile

$$\frac{\rho(r)}{\rho_0} = \left[1 - \frac{(\alpha-1)GM}{r_0 c_{s0}^2}\left(1 - \frac{r_0}{r}\right)\right]^{1/(\alpha-1)} , \tag{3.5}$$

from which the pressure profile is immediately obtained via eq. (3.3):

$$\frac{p(r)}{p_0} = \left[1 - \frac{(\alpha-1)GM}{r_0 c_{s0}^2}\left(1 - \frac{r_0}{r}\right)\right]^{\alpha/(\alpha-1)} , \tag{3.6}$$

and the temperature profile from the equation of state:

$$\frac{T(r)}{T_0} = \left[1 - \frac{(\alpha-1)GM}{r_0 c_{s0}^2}\left(1 - \frac{r_0}{r}\right)\right]^{\alpha} . \tag{3.7}$$

[1] See Appendix E on the polytropic approximation; in a nutshell, in the present context it amounts to assuming a specific solution of the energy equation, including an external source of heating.

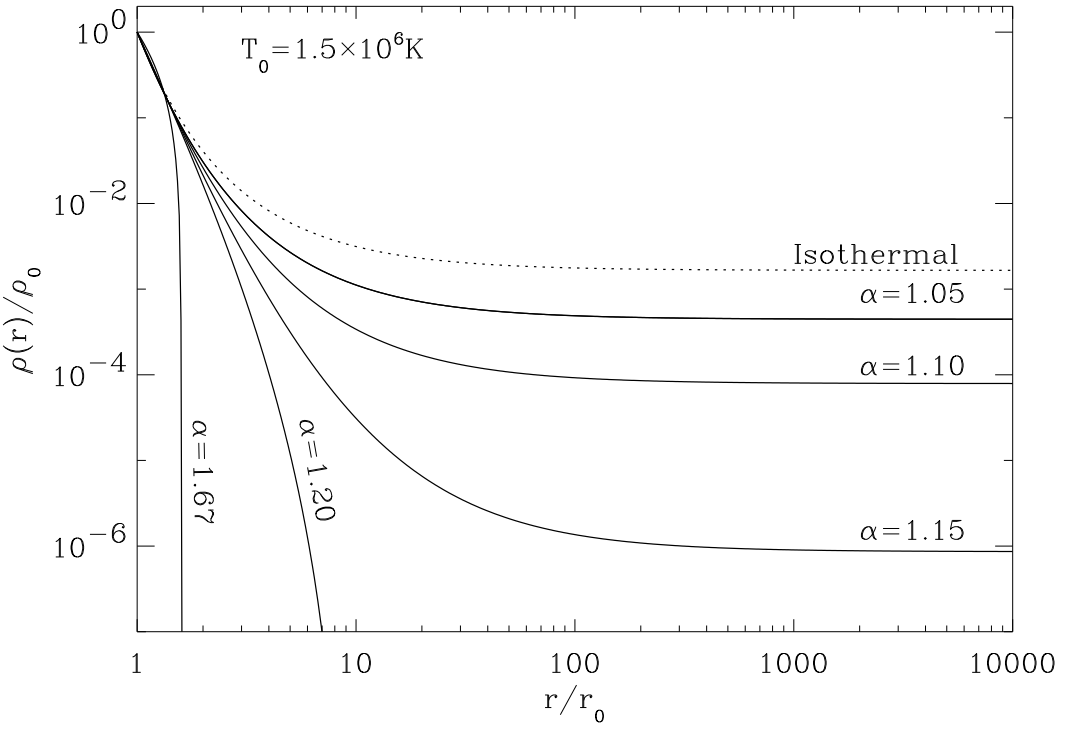

Figure 3.3: Density profiles for a few polytropic static coronal model with $T_0 = 1.5 \times 10^6$ K. and $r_0 = 1.15\,R$. Note the asymptotically constant densities as $r \to \infty$ for $\alpha < 1.1765$.

Examination of these expressions reveals that there may be combinations of T_0 and α values that yield zero pressure and density at a *finite* value of r. Obviously, this occurs whenever

$$c_{s0}^2 < (\alpha - 1)GM/r_0 \ , \tag{3.8}$$

with

$$\frac{r_{\rm top}}{r_0} = \left(1 - \frac{r_0 c_{s0}^2}{(\alpha - 1)GM}\right)^{-1} \tag{3.9}$$

then being the maximum radial extent of the polytropic atmosphere. Eqs. (3.5) through (3.7) describe a static polytropic atmosphere occupying the volume $r_0 \le r \le r_{\rm top}$. For $r > r_{\rm top}$ there is only mathematical vacuum, something Nature abhors, or so Aristotle used to claim. What if T_0 is too large for eq. (3.8) to be satisfied ? Figure 3.3 illustrates a series of polytropic solar coronal models, for $T_0 = 1.5\times10^6$ K, $r_0 = 1.15\,R$, fully ionized hydrogen, and various values of α (for this adopted value of T_0 and for solar parameters, satisfying eq. (3.8) requires $\alpha > 1.1765$). It looks like the solutions that violate eq. (3.8) extend to infinity with non-vanishing pressures and densities. From eq. (3.6) one immediately obtains

$$p_\infty \equiv \lim_{r\to\infty} \frac{p}{p_0} = \left[1 - \frac{(\alpha - 1)GM}{r_0 c_{s0}^2}\right]^{\alpha/(\alpha-1)} \ , \tag{3.10}$$

and similar expressions (with different exponents) for the asymptotic density and temperature. For the parameter values used on Fig. 3.3 and $N_0 = \rho_0/(\mu m_p) = 10^{14}\,{\rm m}^{-3}$, one obtains $N_\infty = 10^{10}\,{\rm m}^{-3}$, $p_\infty \simeq 10^{-7}$ Pa, and $T_\infty = 6 \times 10^5$ K in the $\alpha = 1.1$ case. These values are much larger than anything the interstellar medium has to offer. In the solar galactic neighborhood,

typical densities and temperatures are believed to be $N_{\rm ism} = 10^6\,{\rm m}^{-3}$ and $T_{\rm ism} = 100$ K, so that $p \sim 10^{-15}\,{\rm Pa}$. All of these are insufficient by orders of magnitude[2]. Something is deeply wrong. Given the assumptions made in constructing our simplistic model, four avenues are open to "save" our model:

1. Abandon the hypothesis of a steady-state ($\partial/\partial t = 0$) corona,
2. Work on the energetics to produce a corona with a different asymptotic temperature profile,
3. Abandon the hypothesis of a static ($\mathbf{v} = 0$) corona,
4. Introduce a magnetic field to modify the force balance.

Possibility (1) flies in the face of observations, at least as far as the larger spatial scales are concerned. Early efforts (and efforts to come, as per see problems 3.4 and 3.5...) were mostly directed along avenue (2). Yet avenue (3) proved to be the right one. Avenue (4) produces significant additional improvements to some aspects of the problem, but that will have to await the next chapter. Let's focus on (3) for now.

3.3 Polytropic winds

In this section we will construct a simple, yet reasonably realistic, solar wind model, which will turn out to do a surprisingly good job at reproducing a lot of the large-scale flow properties of the real solar wind. The same underlying physical mechanism turns out to be responsible for the winds emanating from the atmospheres of the polar terrestrial ionosphere, of the atmosphere of other late-type stars, and from the galactic halo. So pay attention to this one.

3.3.1 The Parker Solution

We follow the initial approach of E.N. Parker, in seeking steady state ($\partial/\partial t = 0$) solutions that are spherically symmetric ($\partial/\partial\theta = 0$, $\partial/\partial\phi = 0$). This also implies $u_\theta = 0$, $u_\phi = 0$ (think about it a bit). We *assume* that the star is non-rotating, and surrounded by a hot corona (temperature $\sim 10^6$ K), as in §3.2 extending outward from a reference radius $r = r_0$ where the base temperature (T_0) and density (ρ_0) are assumed known. We seek a wind solution in the domain $r \in [r_0, \infty]$. We consider an inviscid ($\nu = 0$), unmagnetized ($\mathbf{B} = 0$) plasma. We will also limit ourselves to a *single fluid* model. That is, we consider a wind composed exclusively of fully ionized Hydrogen where charge neutrality always holds down to the smallest spatial scales considered[3]. This implies that the proton-electron mixture can be treated as a single fluid, with each particle having a mass μm_p, with $\mu = 0.5$. Once again we make the further simplifying assumption that the flow is *polytropic*, i.e., the pressure and density are assumed to be related by a relation of the form

$$\left(\frac{p}{p_0}\right) = \left(\frac{\rho}{\rho_0}\right)^\alpha \ , \tag{3.11}$$

or, equivalently,

$$\frac{\mathrm{d}}{\mathrm{d}r}\left(\frac{p}{\rho^\alpha}\right) = 0 \ , \tag{3.12}$$

[2] Actually, a realistic estimate of the *total* pressure in the interstellar medium should take into consideration the contribution of the interstellar magnetic field. Far from being negligible, magnetic pressure can provide $\sim 10^{-13}\,{\rm Pa}$ for $\|\mathbf{B}\|_{\rm ism} \sim 1\,{\rm nT}$. But this is still insufficient to equilibrate our hot hydrostatic corona.

[3] Does that also mean that protons and electrons must have identical bulk velocities? Think about that one a bit.

with α constant and specified *a priori* (cf. §1.3). This implies that the sound speed varies with heliocentric radius as

$$c_s^2(r) = c_{s0}^2 \left(\frac{\rho}{\rho_0}\right)^{\alpha-1} , \tag{3.13}$$

where $c_{s0}^2 = \alpha p_0/\rho_0$ is the sound speed at the reference radius. In view of the spherical symmetry assumption, the mass conservation equation reduces to

$$\frac{1}{r^2}\frac{\partial}{\partial r}(r^2 \rho u_r) = 0 , \tag{3.14}$$

which integrates directly to

$$\rho r^2 u_r = \text{const} . \tag{3.15}$$

We only have to deal with the r-component of the equations of motion:

$$\rho u_r \frac{\partial u_r}{\partial r} = -\rho \frac{GM}{r^2} - \frac{\partial p}{\partial r} , \tag{3.16}$$

assuming again a spherically symmetric gravitational potential $\Phi = -GM/r$. Upon making use of eqs. (3.11) and (3.13), equation (3.16) can be manipulated into the form

$$\boxed{\frac{\partial u_r}{\partial r} = \frac{u_r}{r}\left[\frac{2c_s^2 - GM/r}{u_r^2 - c_s^2}\right]} . \tag{3.17}$$

Now, the denominator of eq. (3.17) vanishes when the flow speed becomes equal to the *local* sound speed. This means that the numerator must simultaneoulsy vanish to avoid the appearance of (unwanted) infinite accelerations. The radius r_s at which this occurs is called the *sonic point*, and is located at

$$r_s = \left(\frac{1}{c_{s0}^2}\right)^{2/(5-3\alpha)} \left(\frac{GM}{2}\right)^{(\alpha+1)/(5-3\alpha)} \left(\frac{1}{u_{r0} r_0^2}\right)^{2(\alpha-1)/(5-3\alpha)} , \tag{3.18}$$

where u_{r0} is the base flow speed. At the sonic point we also have

$$u_{rs} = c_s(r_s) = \left(\frac{GM}{2r_s}\right)^{1/2} . \tag{3.19}$$

Now, eq. (3.16) can be rewritten as

$$\frac{\partial}{\partial r}\left[\frac{u_r^2}{2} + \frac{c_s^2}{\alpha - 1} - \frac{GM}{r}\right] = 0 , \tag{3.20}$$

which immediately integrates to

$$\boxed{\frac{u_r^2}{2} + \frac{c_s^2}{\alpha - 1} - \frac{GM}{r} = E} . \tag{3.21}$$

Equation (3.21) is the **Bernoulli equation**, and the integration constant E is the energy per unit mass in the flow. The Bernoulli equation contains the essence of solar wind acceleration: thermal energy of the gas ($c_s^2/(\alpha-1)$) gets converted to gravitational potential energy (GM/r) and flow kinetic energy ($u_r^2/2$), while the total energy is conserved (as it should!). Since the sound speed c_s can be expressed entirely as a function of r and u_r via the mass conservation equation, a solution $u_r(r)$ is then *any* functional $u_r(r)$ satisfying eq. (3.21), for *any* given value of E. But how do we pick an appropriate value for this quantity?

3.3.2 Computing a solution

The key in constructing a wind solution is to realize that any non-singular transsonic solution *must* pass through the sonic point. Let us then begin by writing down expressions for E evaluated at the base of the flow and at the sonic point:

$$E(r_0, u_{r0}) = \frac{u_{r0}^2}{2} - \frac{GM}{r_0} + \frac{c_{s0}^2}{\alpha - 1} \ , \tag{3.22}$$

$$E(r_s, u_{rs}) = -\frac{3GM}{4r_s} + \frac{c_{s0}^2}{\alpha - 1} \left(\frac{u_{r0} r_0^2}{\sqrt{GM/2r_s}\, r_s^2} \right)^{\alpha - 1} \ , \tag{3.23}$$

where we made good use of eq. (3.19). Equating The RHSs of these two expressions yields a nonlinear rootfinding problem for u_{r0}, which can be written schematically as

$$E(r_s, u_{rs}) - E(r_0, u_{r0}) = 0 \ . \tag{3.24}$$

This root finding problem is not particularly easy, in view of the fact that the sonic point r_s itself a nonlinear function of u_{r0} (as per eq. (3.18). The **bisection method** (see Appendix F) is a simple, robust, and easy to code algorithm that works fine here. The solution of eq. (3.24) yields the base flow speed u_{r0} for the transsonic solution, which then allows to compute r_s and E_s. Once u_{r0} is known, computing $u_r(r)$ proceeds by solving a new nonlinear rootfinding problem for u_r defined by setting $E(r, u_r) - E(r_0, u_{r0}) = 0$, with r ($> r_0$) given and r_s now known via eq. (3.18). At this juncture note also that the location of the sonic point is entirely determined by the assumed base sound speed c_{s0} i.e., by the coronal base temperature T_0, and polytropic index α; equally important, u_{r0} is *not* an input parameter of the solution.

With E_s now a fixed quantity, what happens for solutions that start off with different values of u_{r0} and c_{s0}, subjected to the constraint $E(r_0, u_{r0}) = E_s$? Figure 3.4 shows the family of solutions obtained in this manner. There are in fact *two* transsonic solutions (thicker lines) that cross at the sonic point. The accelerating solution is the one we are after for the solar wind. The deccelerating solution has a lower base temperature ($T_0 = 8.7 \times 10^5\,\mathrm{K}$), to compensate for its much higher base flow speed ($u_{r0} = 477.7\,\mathrm{km\,s^{-1}}$). The two transsonic solutions partition the $[r, u_r]$ plane in four distinct regions. Region I correspond to solutions that are supersonic everywhere including at the coronal base; in the solar context, such solutions, as well as the deccelerating transonic solution, conflict with the lack of significant blueshift observed in coronal spectral lines. Regions II and IV do not contain outflow solutions. This leaves the accelerating transsonic solution and solutions in region III as possible valid outflow solutions for the solar wind.

Once $u_r(r)$ is known, it is straightforward to obtain expressions for the density, pressure, and temperature profiles:

$$\frac{\rho(r)}{\rho_0} = \left[1 - \frac{(\alpha - 1)GM}{r_0 c_{s0}^2} \left(1 - \frac{r_0}{r} \right) - \frac{(\alpha - 1)}{2c_{s0}^2} \left(u_r^2 - u_{r0}^2 \right) \right]^{1/(\alpha - 1)} \ , \tag{3.25}$$

$$\frac{p(r)}{p_0} = \left[1 - \frac{(\alpha - 1)GM}{r_0 c_{s0}^2} \left(1 - \frac{r_0}{r} \right) - \frac{(\alpha - 1)}{2c_{s0}^2} \left(u_r^2 - u_{r0}^2 \right) \right]^{\alpha/(\alpha - 1)} \ , \tag{3.26}$$

$$\frac{T(r)}{T_0} = \left[1 - \frac{(\alpha - 1)GM}{r_0 c_{s0}^2} \left(1 - \frac{r_0}{r} \right) - \frac{(\alpha - 1)}{2c_{s0}^2} \left(u_r^2 - u_{r0}^2 \right) \right]^{\alpha} \ . \tag{3.27}$$

Note that these expressions are valid for either the transsonic or class-III solutions. The latter evidently have $\lim_{r \to \infty} u_r \to 0$ (see Fig. 3.4), so that asymptotically, eq. (3.26) becomes identical to eq. (3.10), obtained for a *static* corona! The class-III solutions thus suffer from the same

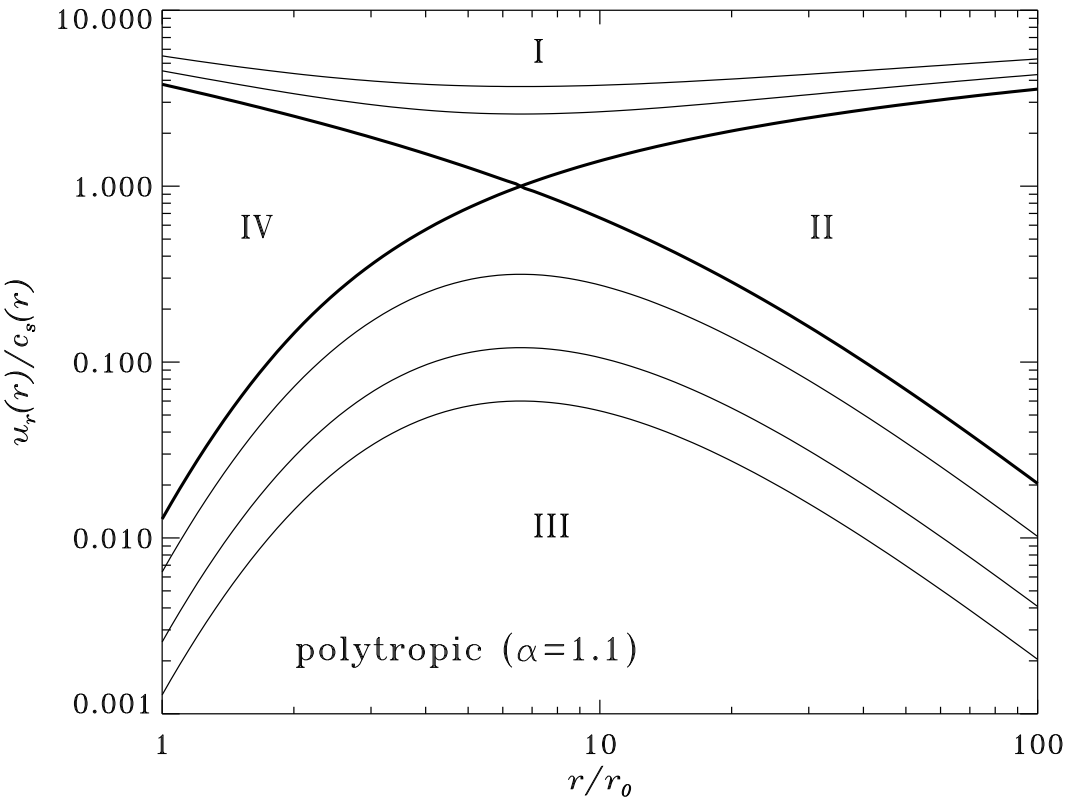

Figure 3.4: Some solutions to equation (3.21). The thick lines are the two transsonic solution satisfying eq. (3.24). The accelerating transsonic solution, to be identified with the solar wind, has a base flow speed $u_{r0} = 2.12\mathrm{km\,s^{-1}}$, sound speed $c_{s0} = 165.1\,\mathrm{km\,s^{-1}}$, with the sonic point located at $r_s/r_0 = 6.59$. The thin lines are solutions for other values of E ($\neq E_s$).

shortcoming: an asymptotic pressure much too high to match that of the interstellar medium, and so can be ruled out.

This leaves us with a single possible outflow solution, namely the accelerating transsonic solutions, which we hereafter refer to as the "wind solution"[4]. Figure 3.5 illustrates the variations with radial distance of the density, pressure and temperature for the transsonic wind solution of Fig. 3.4, together with the corresponding profiles for a $\alpha = 1.1$ polytropic static corona of identical base temperature (dotted lines). Within the sonic point the structure of the solution is very much like that of a static atmosphere, while for $r > r_s$ the solutions differ markedly, reflecting the dynamical effect of the outflow.

3.3.3 Mass loss

One important consequence of the existence of a wind is that it carries away mass from the star. Under the assumption of spherical symmetry used here, the mass loss rate is

$$\dot{M} = 4\pi r_0^2 \rho u_{r0} \ , \qquad [\mathrm{kg\,s^{-1}}] \ . \tag{3.28}$$

For the solar-type solution considered here, $\dot{M} = 10^{-14}\,M_\odot\,\mathrm{yr^{-1}}$, so that over its lifetime the Sun would lose a mere 10^{-4} fraction of its total mass, assuming that this mass loss rate has remained constant since the Sun's arrival on the Zero-Age Main-Sequence (ZAMS); as we shall see later, there are good reasons to believe that the ZAMS mass loss rate may have been substantially higher.

[4]Traditionally, class-III solutions have been dubbed "solar breeze", since the flow speed they predict at the Earth's orbit is much smaller than for the wind solution

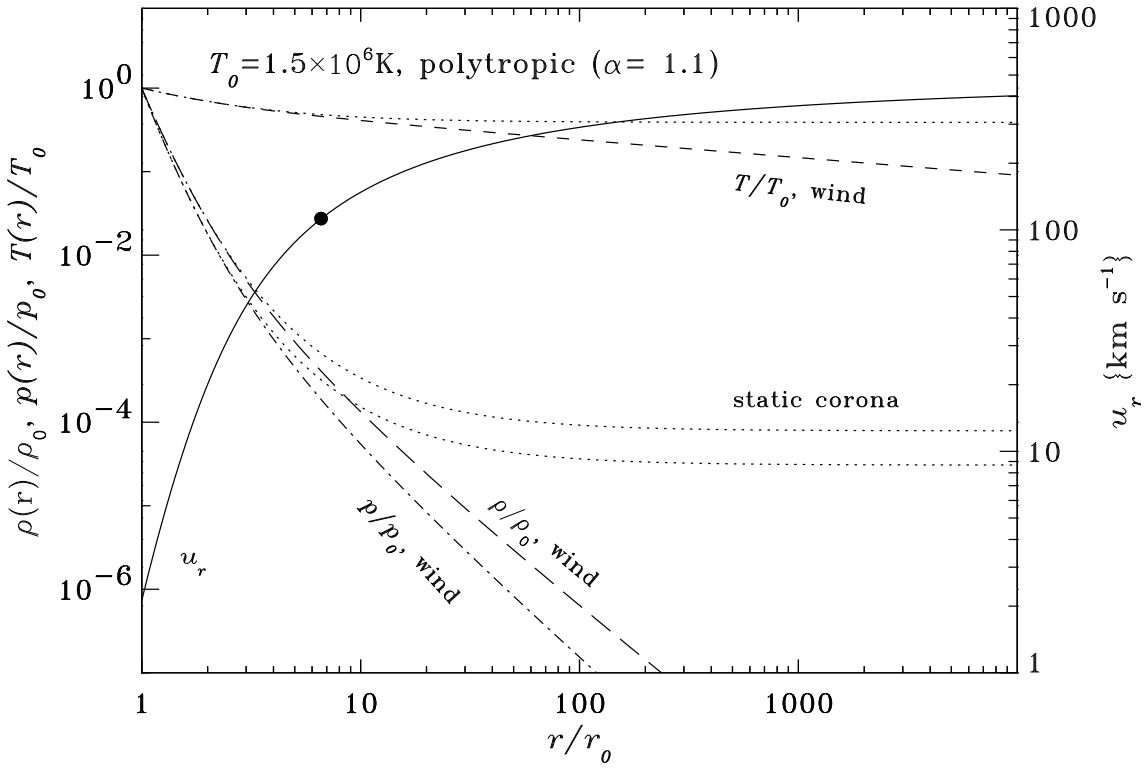

Figure 3.5: The full wind solution corresponding to the accelerating transsonic solution of Fig. **??**. Dotted lines correspond to a polytropic static coronal model with identical α and T_0. The solid dot indicates the location of the sonic point.

3.3.4 Asymptotic behavior and existence of wind solutions

To analyze the asymptotic behavior of the wind solution we do something undoubtedly familiar by now: we equate $E(r, u_r)$ evaluated at r_0 and in the limit $r \to \infty$:

$$\frac{u_{r0}^2}{2} - \frac{GM}{r_0} + \frac{c_{s0}^2}{\alpha - 1} = \lim_{r\to\infty} \left[\frac{u_r^2}{2} - \frac{GM}{r} + \frac{c_{s0}^2}{\alpha - 1} \left(\frac{u_{r0} r_0^2}{u_r r^2} \right)^{\alpha - 1} \right] . \tag{3.29}$$

Now, what the wind solution does is convert all thermal energy in excess of what is needed to climb out of the Sun's gravitational potential well into bulk flow kinetic energy. This implies $u_r \gg c_s$ asymptotically. Furthermore, we also have $\lim_{r\to\infty} u_r \gg u_{r0}$ and $u_{r0} \ll c_{s0}$, so that eq. (3.29) readily yields

$$\lim_{r\to\infty} u_r \equiv u_{r\infty} = \left(\frac{2c_{s0}^2}{\alpha - 1} - \frac{2GM}{r_0} \right)^{1/2} . \tag{3.30}$$

indicating that the flow speed becomes constant at large r.

Clearly all wind solutions must have $u_{r\infty} > 0$ for finite r, so that we have the constraint[5]:

$$\frac{c_{s0}^2}{\alpha - 1} - \frac{GM}{r_0} \geq 0 . \tag{3.31}$$

[5]Why is that so ? What's wrong with a steady, spherically symmetric wind accelerating in the corona and then, at some large distance, deccelerating again until everything grinds to a full stop ?

For $\alpha = 1.1$, this requires that $T_0 \gtrsim 9 \times 10^5$ K. An accelerating transsonic solution also requires $\mathrm{d}u_r/\mathrm{d}r > 0$ near the base of the flow. Going back to eq. (3.17), this implies

$$2c_{s0}^2 - \frac{GM}{r_0} < 0 \ , \tag{3.32}$$

requiring that $T_0 \lesssim 5 \times 10^6$ K. So a transsonic wind can only exist for a base temperature in the range

$$\left(\frac{\alpha - 1}{\alpha}\right) \frac{GM\mu m_p}{kr_0} \leq T_0 < \left(\frac{1}{2\alpha}\right) \frac{GM\mu m_p}{kr_0} \tag{3.33}$$

What do these two bounds on T_0 correspond to physically? The lower bound is simply the criterion for the existence of a gravitationally bound atmosphere, which we encountered already in §3.2, in fact. The upper bound is trickier to interpret. It represents the temperature above which steady, transsonic wind solutions no longer exist. If this criterion were to be violated (e.g. by a sudden increase in base temperature), the whole atmosphere would "explode" outward in a very time-dependent manner. You may think of this as a very simple-minded explanation of flares, although in reality there is much more to it than that.

There is something else that is extremely important that can be extracted from eq. (3.33); if there is to be a finite temperature interval over which it is to be satisfy, then we *must* have $\alpha > 3/2$. Otherwise both criteria cannot be satisfied simultaneously. We therefore have the additional constraint $1 \leq \alpha \leq 3/2$, independently of the assumed base temperature T_0.

Figure 3.6 illustrates, in the $[T_0, \alpha]$ plane, the region in parameter space where steady, transsonic solutions are allowed. The thermodynamically allowed bounds on α ($\leq \alpha \leq 5/3$ for a perfect monoatomic gas) restrict solutions to the region located below the dotted line. Equation (3.31) (finite asymptotic flow velocity) restricts solution to the right of the dash-dotted line. Equation (3.32) (subsonic, accelerating flow at r_0) restricts solutions to the leff of the dashed line. So our allowed region is that labeled "II". Region I is that of steady hydrostatic coronae of finite radial extent, discussed in §3.2. In region III no steady wind-type solution is possible.

3.3.5 Energetics

As discussed in Appendix E, buried deep in the polytropic approximation (i.e., eq. [3.11] with α a constant specified *a priori*) is a very specific energy source/sink functional form. We now have pretty good solution, in terms of its asymptotic behavior, etc., but must now ask ourselves whether or not this solution involves distributions of energy sources/sinks that are even mildly reasonable.

Now our solutions, in general, will not satisfy the energy equation (which we didn't solve for anyway, having effectively *replaced* it by the polytropic approximation). But we can turn the issue around and use our solution to determine what sources/sinks *should* appear on the RHS of the energy equation in order for our solution to satisfy it. Neglecting thermal conduction and limiting ourselved to steady-state ($\partial/\partial t = 0$) systems, the energy equation can be manipulated into the form

$$\nabla \cdot \left[\rho \mathbf{u} \left(\frac{1}{2}\|\mathbf{u}\|^2 + \frac{3}{2}\frac{p}{\rho}\right)\right] + \nabla \cdot (p\mathbf{u}) - \rho \mathbf{u} \cdot \nabla\Phi = s(r), \tag{3.34}$$

where $s(r)$ is our extraneous volumetric source/sink term (which has units of J s^{-1} m^{-3}), artificially added on the RHS. Direct substitution of our polytropic solutions on the LHS of this expressions allows to calculate directly the functional form of the heating term $s(r)$ so that the energy equation is now satisfied by construction. Figure 3.3.5 shows the resulting $s(r)$, for a sequence of solution having $T_0 = 1.5 \times 10^6$ K and different values of α. The *total* energy input associated with our source is

$$S(\alpha, T_0) = 4\pi \int_{r_0}^{\infty} s(\alpha, T_0; r) r^2 \mathrm{d}r. \qquad [\mathrm{J\ s^{-1}}] \tag{3.35}$$

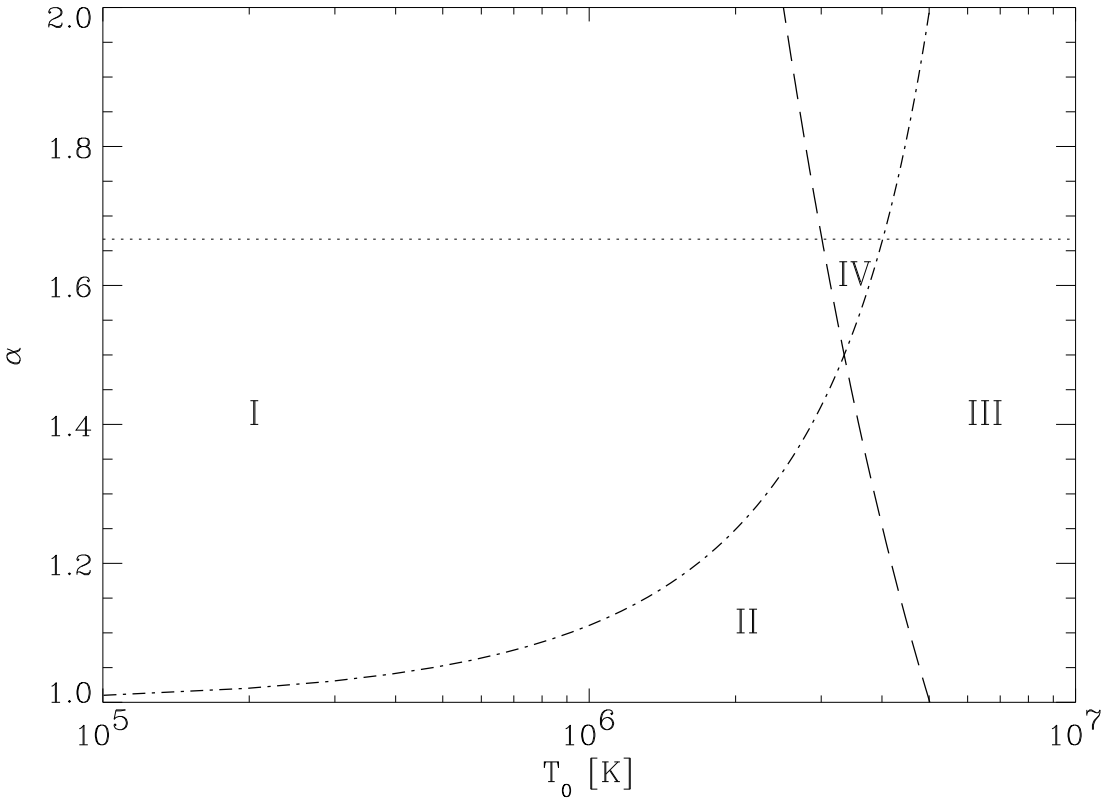

Figure 3.6: Allowed region in the $[T_0, \alpha]$ plane for the existence of steady, transsonic polytropic wind solutions. The region $\alpha > 5/3$ is thermodynamically excluded. Region II is the allowed region, as defined by eq. (3.33) (see text). Note that the I—IV labeling of regions is unrelated to the similar labeling on Fig. 3.4.

Carrying out this integral yields $S = 1.1 \times 10^{21}$, 2.3×10^{20}, and 8.7×10^{19} J s^{-1} for $\alpha = 1.05$, 1.1, and 1.15 respectively; in all cases, this is less than 10^{-5} of the solar luminosity, a fortunate state of affairs. Likewise, it is reassuring that the heating term peaks at the coronal base and decreases rapidly outward, since the heating ultimately originates near the solar surface.

3.3.6 Comparison with the Solar Wind

Time to compare our polytropic solutions to the real solar wind. Flow properties at 1 AU for the solution of Fig. 3.5 are listed in Table 3.2 below. Compare this to Table 3.1, in particular to the flow properties of low speed streams. Pretty amazing; our model values are within the observed fluctuations for the flow speed, *and* particle number density. We are off by a whopping factor of 10 on the temperature (the proton temperature should be the meaningful one to compare to in the context of our single-fluid model), but the fact that the observed temperatures for protons, electrons and Helium nucleii differ by large factors (cf. Table 2.1) is telling us (very loudly) something about the breakdown of our single fluid approximation.

Table 3.2
Parker's solar wind solution

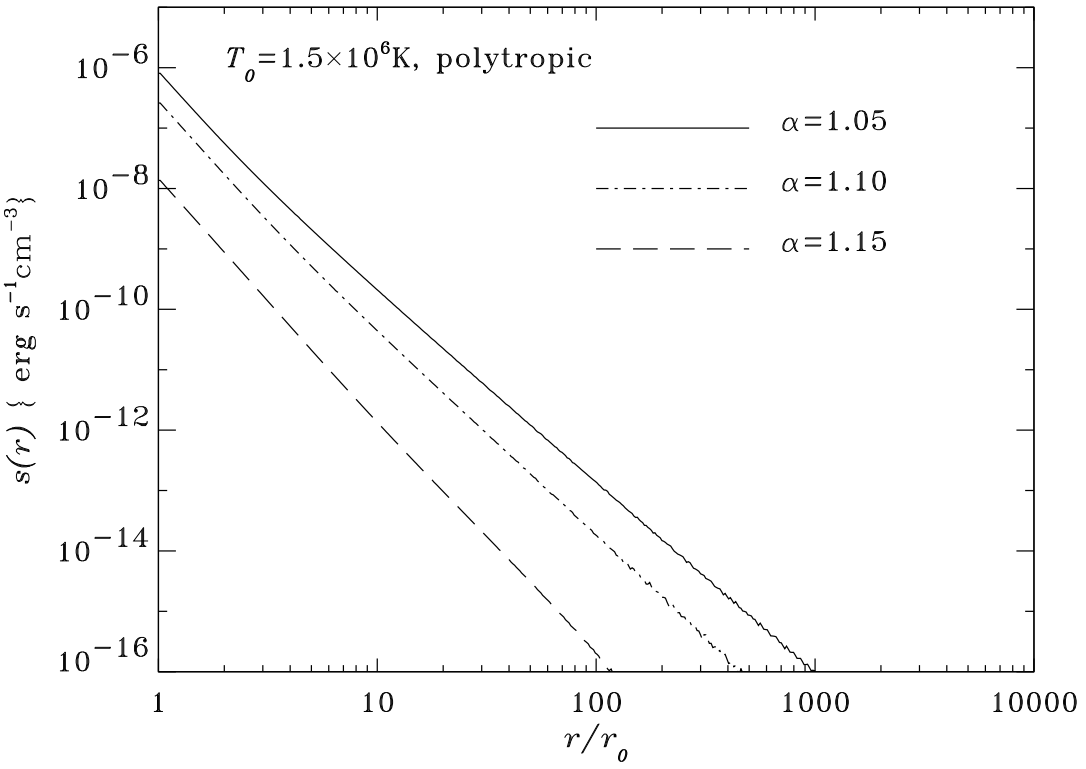

Figure 3.7: Energy input implicit in the polytropic wind solutions, for a few values of α. The base temperature is $T_0 = 1.5 \times 10^6$ K in all cases.

r	u_r [km s^{-1}]	N [10^6 m^{-3}]	T [K]
r_0	2.1	10^8	1.5×10^6
r_s	113	4×10^4	6.8×10^5
$r_\oplus$	315	16	3.1×10^5
$10\,r_\oplus$	377	0.12	1.9×10^5

This leaves unexplained the higher speeds and lower densities observed in high speed streams. Within the framework of the thermally-driven models discussed here, a large increase in the asymptotic flow velocity can only be generated by increasing the base temperature. This being generally ruled out by observations, a number of authors have attempted to "speed up" the solar wind at 1 AU. One way of doing so is by introducing additional sources of energy and/or momentum at various distances from the base of the corona. An important and very robust result in that context is that

- Adding momentum or energy in the subsonic ($r < r_s$) region increases the overall mass flux, but not the flow speed at 1 AU.

- Adding momentum or energy in the supersonic ($r > r_s$) region increases the flow speed at 1AU, but not the overall mass flux.

Nice and fine, but how do we achieve that? Guess what, magnetic fields can do the trick, both in indirect and direct ways. This is the focus of the following two chapters.

Problems:

1. Obtain eqs. (3.18)—(3.19)
2. Obtain eqs. (3.25)—(3.27)
3. Assuming that the Sun's present mass loss rate has remained constant since its arrival on the ZAMS, calculate by how much the Sun-Earth distance has varied over the past 4.5 Gyr.
4. The purpose of this problem is to get you to construct a coronal model that is more realistic, energetically speaking, than the isothermal and polytropic models discussed in §3.2. Your starting point is the assumption that *thermal conduction* dominates the energy transport in the corona. For a static and steady-state corona, the energy equation then reduces to

$$\nabla \cdot (\chi \nabla T) = 0.$$

where χ is the coefficient of thermal conductivity. In a low density, high temperature plasma of fully ionized hydrogen, an approximate (yet fairly accurate) expression for κ is

$$\chi(T) = \chi_0 T^{5/2},$$

where $\chi_0 \simeq 8 \times 10^{-13}$ J m^{-1} s^{-1} K$^{-7/2}$. So your task is the following:

   (a) Obtain expressions for $T(r)$, $\rho(r)$, and $p(r)$, and plot these as a function of r for a few values of T_0 in the range $10^6 \leq T_0 \leq 5 \times 10^6$ K.

   (b) Obtain asymptotic ($r \to \infty$) expression for $T(r)$, $\rho(r)$ and $p(r)$, and calculate these asymptotic values for the solutions you obtained in (a)

   (c) Compare and contrast your results in (b) with the corresponding results for the polytropic coronae discussed at the end of this chapter.

   (d) What is the energy input (J s^{-1}) require to maintain the corona in its assumed steady state, given the outward transport of energy? Can you think of other important coronal energy "sinks"?

5. This problem further explores possible "fixes" for our static coronal models.

   (a) Determine how fast the temperature profile would have to fall with distance for the pressure to vanish at infinity in a static corona.

   (b) What should be the coronal temperature for a static, *isothermal* corona to by dynamically balanced by the pressure in the interstellar medium?

   (c) How strong a magnetic field in the interstellar medium would be needed to balance the asymptotic pressure of our static coronae models? Can you think of one known observations that rules this out?

6. Code in the pseudocode for the bisection method, as given in the text, to reconstruct (and plot) a full polytropic wind solution (i.e. $u_r(r)$, $\rho(r)$, $p(r)$ and $T(r)$). Keeping the polytropic index fixed at $\alpha = 1.1$, examine how the sonic point location, base flow speed, and wind properties at 1 AU vary with base temperature, in the range $10^6 \leq T_0 \leq 2 \times 10^6$ K. And please do provide a listing of your code.
7. This problem lets you construct an *isothermal* solar wind solution. Upon examination of the expressions we obtained for the polytropic model, one rapidly sees that simply setting $\alpha = 1$ leads to divergence, so you actually need to start from scratch;

(a) Using the definition of the isothermal sound speed $a^2 = p/\rho$, obtain the isothermal equivalents of eqs. (3.17) and (3.21).

(b) Obtain an expression for the location of the sonic point in terms of a and other model input quantities.

(c) Construct a transsonic wind solution for $T_0 = 1.5 \times 10^6\,\mathrm{K}$; compare its base flow speed, sonic point location, and speed and densities at Earth's orbit with the corresponding quantities for the polytropic solution of §3.3.

(d) Obtain an expression for the asymptotic flow speed, i.e., the isothermal equivalent of eq. (3.30). How can you explain your (presumably surprising) result?

8. Using the procedure outlined in the text, construct a numerical solution corresponding to a class III polytropic solution (i.e., subsonic for all r, cf. Fig. 3.1; use also $\alpha = 1.1$ and $T_0 = 1.5 \times 10^5\,\mathrm{K}$). Provide plots of the flow speed, density, pressure and temperature as a function of r. Examine the asymptotic ($r \to \infty$) behavior of your solution, and discuss its physical relevance.

Bibliography:

The first reasonable models for hydrostatic coronae were constructed by

Chapman, S. 1957, Smithsonian Contrib. Ap., 2, 1.

Evidence for the existence of ionized gas (static or not) in the interplanetary environment was first infered on the basis of the measured polarization of zodiacal light. The classic reference is

Behr, A., & Siedentopf, H. 1953, *Zeitschrift Ap.*, **32**, 19.

On circumstantial evidence for the present of a continuous outflow from the Sun, based on comet tail acceleration, see

Biermann, L. 1951, *Zeitschrift Ap.*, **29**, 274.

Parker's original paper on the topic is a great lesson in how to do good physics starting from simple assumptions, and should not be missed:

Parker, E.N. 1958, *Astrophys. J.*, **128**, 664

The Web site of the *Ulysses* mission is also well worth looking at:

`http://ulysses.jpl.nasa.gov`

The effect of additional energy/momentum sources in the corona on the solar wind is investigated in

Leer, E., & Holzer, T.E. 1980, JGR, 85, 4681

For a thorough, recent review of MHD waves and wave-particle interaction in the solar corona and wind, see

Marsch, E. 2006, Liv. Rev. Sol. Phys., 3, 1
`http://solarphysics.livingreviews.org/Articles/lrsp-2006-1`

The following is a relatively recent and noteworthy monograph on stellar winds:

Lamers, H.G.L.M., et Cassinelli, J.P., *Introduction to Stellar Winds*, Cambridge University Press (1999).